PHYSICAL REVIEW B **90**, 201302(R) (2014)

Polariton path to fully resonant dispersive coupling in optomechanical resonators

G. Rozas,[1] A. E. Bruchhausen,[1] A. Fainstein,[1,*] B. Jusserand,[2] and A. Lemaître[3]
[1]*Centro Atómico Bariloche and Instituto Balseiro, C.N.E.A., 8400 S. C. de Bariloche, R. N., Argentina*
[2]*Institut des NanoSciences de Paris, UMR 7588 C.N.R.S.–Université Pierre et Marie Curie, 75015 Paris, France*
[3]*Laboratoire de Photonique et de Nanostructures, C.N.R.S., 91460 Marcoussis, France*
(Received 1 May 2014; revised manuscript received 3 October 2014; published 3 November 2014)

Resonant photoelastic coupling opens new perspectives for strongly enhanced light-sound interaction in semiconductor optomechanical resonators. One potential problem, however, is the reduction of the cavity Q factor induced by dissipation when the resonance is approached. We show in this Rapid Communication through Raman-scattering experiments that cavity-polariton mediation in the light-matter process overcomes this limitation allowing for a strongly enhanced photon-phonon coupling without significant lifetime reduction in the strong-coupling regime. Huge optomechanical coupling factors in the petaHz/nm range are envisaged, three orders of magnitude larger than the backaction produced by the mechanical displacement of the cavity mirrors.

DOI: 10.1103/PhysRevB.90.201302 PACS number(s): 78.20.hb, 78.30.Fs, 78.67.De, 78.67.Pt

Optomechanical resonators have emerged as novel paradigms for new fundamental ideas and applications [1–11]. Light-induced rigidity, optomechanical cooling down to the quantum ground state of mechanical motion [12–15], and optomechanical self-oscillation [16,17] are some of the demonstrated consequences of so-called dynamical backaction in these devices. Very recently hybrid systems combining cavity optomechanics and cavity quantum electrodynamics (CQED) have been theoretically proposed as a means to evidence unconventional dissipative couplings and cooling at the single-polariton level [18,19]. Here we experimentally demonstrate using resonant acoustic phonon Raman scattering the possibility to access in CQED optomechanics a hugely enhanced optomechanical coupling of dispersive photoelastic resonant nature, without significant dissipation-induced cavity Q-factor quenching.

Dynamical backaction in cavity optomechanical devices relies on the possibility to strongly couple photons and phonons in resonators of large optical and mechanical Q factor. "Radiation pressure" is usually identified as the main origin of optomechanical coupling. Direct transfer of impulse from the photon field to the resonator mirrors induces vibrations on the latter, which in turn results in a backaction on the optical cavity mode due to the mechanical displacement of the mirrors. Alternative stronger optomechanical coupling mechanisms are also being sought [20–26]. We have recently reported that GaAs Distributed Bragg Reflector (DBR)-based microcavities constitute optimized optomechanical resonators operating in the GHz-THz range [27,28], with the potential for adding an additional photoelastic term to the above described purely "mechanical" mechanism [24]. The two complementary sides of the coin in this case are electrostriction, and as backaction, the phonon-induced modulation of the dielectric function [24,25]. Under resonant conditions the photoelastic mechanism in GaAs (and similar materials) [29–31] should become dominant, allowing for huge optomechanical coupling factors [24].

A resonant enhancement of dispersive photoelastic coupling is, however, typically related to dissipation. At the electronic gap the photoelastic constants resonate, but also at the gap strong absorption sets in, and thus the optical cavity Q factor should be quenched. Indeed this is critical for bulk-GaAs cavities, as illustrated in Fig. 1 where we show the photoelastic constant of GaAs, and the optical Q factor of a bulk-GaAs $\lambda/2$ microcavity close to resonance with the fundamental E_0 gap. Photons absorbed through the creation of electron-hole pairs are irreversibly lost into the band continuum, resulting in the observed strong reduction of cavity Q factor. There is an enormous potential to exploit photoelastic coupling in resonant materials in the domain of cavity optomechanics, but in order to do that dissipative Q factor quenching needs to be avoided.

The interaction of light with a *discrete* electronic state instead of a continuum would result in reversible coupling. Excitons in semiconductors have discrete spectra and could be an alternative in this direction. While in bulk GaAs and at room temperature excitons are not stable, they do define the optical properties of quantum wells (QWs) because of the larger binding energy and oscillator strength induced by confinement [32]. However, in real samples absorption can be broad and lossy anyway due to roughness and inhomogeneous broadening. This leads, for microcavities with embedded collections of QWs in the "weak-coupling regime," to a general behavior similar to that displayed in Fig. 1.

We propose here that the situation is qualitatively modified when the "strong-coupling regime" is considered [33–35]. Cavity polaritons, the quasiparticles that define the strong-coupling regime, provide the solution to the posed problem for the following reasons: (i) inhomogeneous broadening becomes irrelevant in the strong-coupling regime. In fact a *single* linear combination of the set of exciton states couples to the electromagnetic field. In addition, this coupled polariton mode is redshifted into the transparency region of the material, out of the spectral region were a continuum can lead to irreversible loss. The remaining $N-1$ remain as uncoupled optically "dark" states [36,37]. Moreover, (ii) polaritons allow for extended lifetimes because the dressed states bounce back and forth from exciton to photonic character before the excitation can dephase through the more dissipative channel [38], and (iii) polariton mixing leads to much smaller masses, leading to spatial averaging over the disorder potential and hence motional narrowing of the spectral lines [39]. The consequence

*afains@cab.cnea.gov.ar

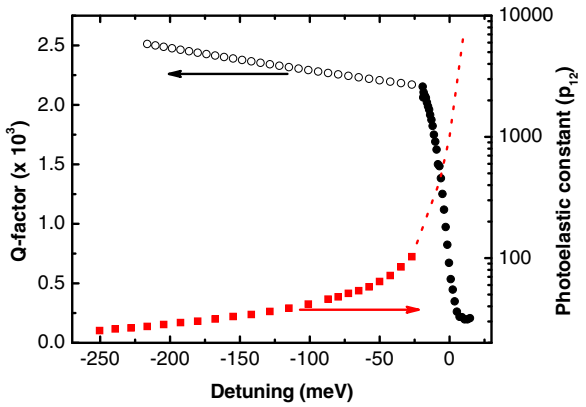

FIG. 1. (Color online) Right scale: Photoelastic constant as a function of the detuning between the laser energy and the E_0 gap of GaAs (from Refs. [29,31]). Left scale: Optical cavity Q factor for a $\lambda/2$ GaAs resonator. Symbols in the photoelastic constant correspond to data derived from piezobiregringence experiments, [29] and the dotted curve is a schematic behavior derived from recent predictions based on Brillouin scattering data [30,31]. The solid symbols in the Q factor correspond to measured values, while open symbols are extrapolated assuming no additional mode broadening in the transparency region of GaAs.

is that polariton states are characterized by a *homogeneous* broadening, which in high-quality samples can result in Q factors in the 10^4 range.

We will evaluate the optomechanical photoelastic coupling and the optical Q factor under polariton excitation in an optical microcavity by studying the Raman efficiency for the optical generation of hypersound [40,41]. The sample is a planar microcavity with $Al_{0.3}Ga_{0.7}As/AlAs$ (61.17/71.21 nm) DBRs—20 pairs in the bottom, 16 pairs on top. Because resonant Raman experiments involving the 20 GHz fundamental optomechanical mode of the microcavity are presently unaccessible [42], we will concentrate this investigation on higher frequency 250 GHz acoustic phonons confined in an acoustic multilayer performing as a microcavity spacer [43,44]. The latter consists of a 32-period GaAs/AlAs (14.16/5.81 nm) multiple quantum well (MQW). The experiments have been performed in resonance around the GaAs exciton of these MQWs at 1.53 eV. The optical microcavity has a thickness gradient that allows for the tuning of the cavity mode in the vicinity of this energy.

Figure 2 (top) shows with solid symbols the measured polariton energies as a function of cavity-heavy-hole exciton detuning δ_H [41], together with a simultaneous fit of all three polariton branches, with eigenstates of the form [33–35] $|P\rangle = A_C^P(\delta_H)|C\rangle + A_H^P(\delta_H)|H\rangle + A_L^P(\delta_H)|L\rangle$. The coefficients $S_C^P = |A_C^P|^2$, $S_H^P = |A_H^P|^2$, and $S_L^P = |A_L^P|^2$, shown in Fig. 2 (bottom) for the lower and middle polaritons, describe the strength of the cavity-, heavy-, and light-hole excitonic states, respectively, on the dressed polariton states. P stands for the lower (LP), middle (MP), and upper (UP) polariton branches, respectively. The modulation of such cavity-polariton states by externally injected phonon pulses and surface acoustic waves has been investigated in Refs. [45–47]. In what follows we will demonstrate that they provide the means to channel the strongly efficient resonant

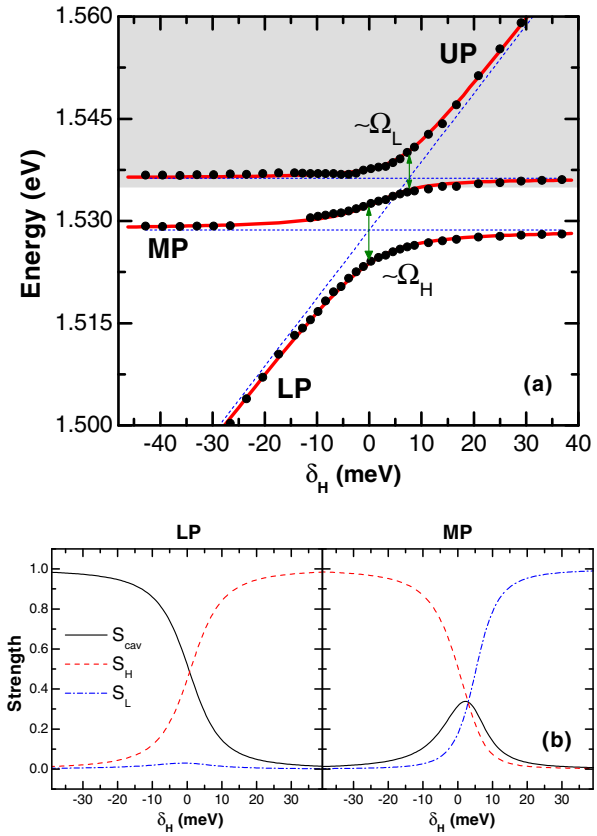

FIG. 2. (Color online) (a) Polariton energies (solid symbols) and fitted dispersion (continuous curves) as a function of cavity-heavy-hole exciton detuning (δ_H). LP, MP, and UP indicate the lower, middle, and upper polariton branches, respectively. $\Omega_H \approx 9.1$ meV and $\Omega_L \approx 5.9$ meV are the heavy- and light-hole Raby splittings, respectively. The uncoupled exciton states and cavity mode are indicated with dotted curves. The gray background marks the continuum of e-h excitations. (b) LP and MP photonic and excitonic strength as a function of δ_H.

optical excitation of mechanical vibrations in the context of cavity optomechanics, without dissipative quenching of the optical Q factor.

Figure 3 summarizes the main results of this paper. Experimental Raman intensities as a function of δ_H are displayed as color maps for a double resonant configuration with both the laser and collected photons tuned along each of the three polariton branches. Experiments were performed at 80 K in quasidouble resonance, with light collected normal to the sample, and the laser incident with $\approx 5^\circ$ [48,49]. The detuning is varied by shifting the spot position on the sample and adjusting the laser energy to the corresponding local polariton energy, following thus the curves in Fig. 2(a). Typical Raman spectra corresponding to folded acoustic modes with energies around 8 cm^{-1} (or 250 GHz) are shown at the left panels for the maximum integrated intensity of each polariton branch [44,48]. Modes normally seen in Raman experiments using forward and backscattering configurations [50] are simultaneously observed in microcavities [51–53] due to the standing-wave character of the confined electromagnetic field (see Ref. [41] for a detailed analysis of the spectra). The larger Raman intensity concentrates close to the branch's

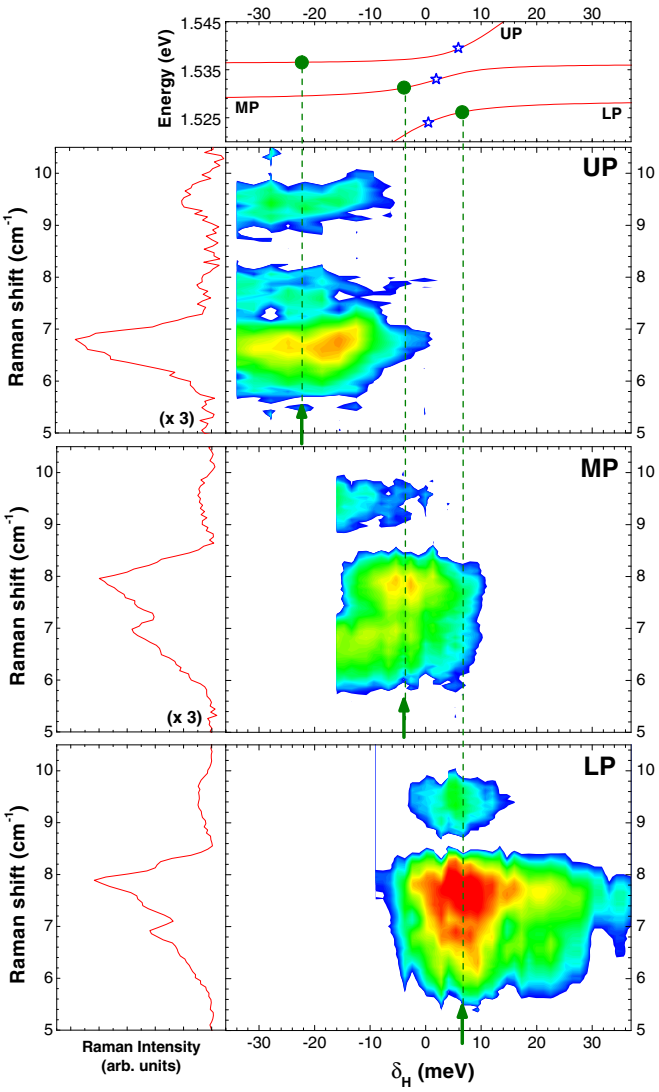

FIG. 3. (Color online) Experimental Raman intensity maps as a function of δ_H, for the three polariton branches. The color scale is logarithmic, with red the most intense Raman cross section. The top panel shows the calculated polariton dispersion. Open stars indicate the expected condition for maximum Raman efficiency, without account of lifetime effects. Left panels present the Raman spectra obtained at the maximum integrated intensity for each polariton branch, labeled with a vertical arrow in the corresponding map.

anticrossing, that is, when polaritons display similar excitonic and photonic character.

To proceed further in a more quantitative description of the experimental observations we next present the model of Raman scattering mediated by polaritons [41]:

$$I_R(E_s) \propto T_i\, \tau_i\, |\langle P_i|\mathcal{H}_{EF}(\omega_{\rm ph})|P_s\rangle|^2\, T_s\, \rho_s \times \delta(E_i - \hbar\omega_{\rm ph} - E_s). \quad (1)$$

Here $|P_i\rangle$ and $|P_s\rangle$ are the initial and final polariton states, with energies E_i and E_s, respectively. The lifetime of the initial state is τ_i, while ρ_s represents the final density of states [40,54–57]. A photon of energy E_i impinges on the material's surface and is converted into a polariton P_i with probability T_i. Before dephasing by relaxation processes occurring in a typical time τ_i, the polariton P_i interacts with the lattice through the Hamiltonian H_{EF} (photoelastic coupling), creating or annihilating an acoustic phonon of energy $\hbar\omega_{\rm ph}$. Finally, the scattered polariton P_s leaves the system with a probability T_s.

Equation (1) for the LP can be expressed in a simpler form for intrabranch scattering using the previously defined photon and exciton strengths [41]:

$$I_R^{\rm LP} \propto S_C^{\rm LP\,2}\left(S_H^{\rm LP\,2} + \alpha_L^2 S_L^{\rm LP\,2}\right)\Gamma_{\rm LP}^{-2}. \quad (2)$$

To derive Eq. (2) the probability for an external photon to couple with a polariton is taken as proportional to the photon strength of the latter, $T_{\rm LP} \propto S_C^{\rm LP}$. $\tau_{\rm LP}$ is determined by the *homogeneous* spectral width of the involved polariton state, $\Gamma_{\rm LP} = \tau_{\rm LP}^{-1}$. $\rho_{\rm LP}$ is also proportional to $\Gamma_{\rm LP}^{-1}$. The polariton width is $\Gamma_{\rm LP} = \Gamma_C S_C^{\rm LP} + \Gamma_H S_H^{\rm LP} + \Gamma_L S_L^{\rm LP}$, with Γ_C, Γ_H, and Γ_L the *homogeneous* spectral widths of the cavity mode, and the two involved exciton states, respectively. The electron-phonon Hamiltonian matrix element has been expressed as [41] $|\langle {\rm LP}|\mathcal{H}_{EF}|{\rm LP}\rangle|^2 \propto S_H^{\rm LP\,2} + \alpha_L^2 S_L^{\rm LP\,2}$ with $\alpha_L = \langle L|\mathcal{H}_{EF}|L\rangle/\langle H|\mathcal{H}_{EF}|H\rangle$. This equation expresses the fact that polaritons interact with the lattice only through their exciton component. It is in Eq. (2) that the two central concepts of this work are captured: First, the quadratic dependence on S_X expresses the strong double-resonant photoelastic interaction, and secondly a smoothly behaved and narrow $\Gamma_{\rm LP}$ reflects the fact that the LP mode's linewidth (i.e., its Q factor) is determined by the homogeneous broadening of cavity and exciton modes, and is *not* significantly altered by losses. Similar equations can be derived for the other two polariton branches.

To be optimized Eq. (2) requires a simultaneous maximization of the photonic and excitonic strengths of the participating polaritons. If the photon component dominates, light will couple efficiently with the material polaritons, but the latter will couple poorly with the lattice. A large exciton strength of the polariton assures a strong interaction with phonons, but a poor coupling efficiency with the outside world. The optimum hence should occur when exciton and photon strengths are similar, that is, close to zero cavity-exciton detuning [open stars in Fig. 3 (top)]. The maxima of the Raman efficiencies for all three branches fall close to these values, but are somewhat shifted towards detunings corresponding to larger excitonic character on each branch. This effect derives from lifetime effects in Eq. (2), as we discuss next.

In Fig. 4 (bottom) we present with solid symbols the Raman intensity (integrated over the full Raman spectra) as a function of δ_H measured for the lower (left) and middle (right panel) polariton branches. Let us first address the LP case. The dashed curve corresponds to a simpler form of Eq. (2) $I_R \propto S_C^i S_X^i S_X^s S_C^s$, i.e., without inclusion of lifetime effects. Besides a rigid redshift of the curve with respect to the experiment, it is quite notable the resemblance, particularly when the *only* adjustable parameter in this calculation is the maximum intensity. The blueshift of the data with respect to the calculation is indicative of lifetime effects. In fact, according to Eq. (2) the resonance scan maxima should shift either towards more photonic or excitonic character, depending on whether the cavity confined photon or the exciton, respectively, have a longer lifetime. The continuous curve in Fig. 4 (bottom left) corresponds to the full calculation using Eq. (2). Here we have used the measured linewidth of the

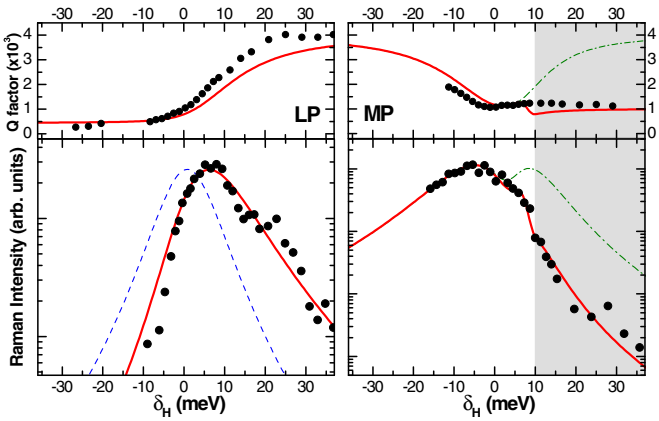

FIG. 4. (Color online) Bottom panels: Total Raman integrated intensity as a function of cavity-E_1H_1 detuning for the lower (left panel) and middle (right panel) polariton branches. Curves are obtained using Eq. (2) (see text for details). Note the logarithmic scale. Top panels: Corresponding cavity polariton mode Q factor for each branch derived from the fit of the Raman intensities. Solid circles are independent experimental values estimated from the photoluminescence linewidths. Gray regions indicate the continuum of e-h excitations.

cavity mode obtained in the pure photonic regime ($\Gamma_C \sim 3.3$ meV, i.e., a cavity Q factor $\sim$450), corresponding to a lifetime $\tau_C \sim 0.2$ ps. The only fitting parameters are the maximum Raman intensity, and the ratio Γ_C/Γ_H. The H-exciton lifetime that is obtained from the fit is $\sim$1.8 ps (corresponding to $\Gamma_H \sim 0.4$ meV homogeneous linewidth, as compared to $\sim$1.1 meV inhomogeneous broadening measured at very negative detunings), which is reasonable for a GaAs MQW at 80 K. The agreement is remarkable. The Q factor derived from the fit of the Raman intensity using the polariton model is shown with a full line on the top panel in Fig. 4 (left). As an additional test for the model, an estimation of the cavity polariton mode Q factor obtained from the measured photoluminescence linewidths is shown with full circles. Note the contrast with the situation depicted in Fig. 1 for bulk GaAs. The cavity Q factor nicely follows the predicted behavior, related to the *homogeneous* linewidth of the polariton. For the strongly coupled cavity structure studied here, with $\Gamma_C > \Gamma_H$, the Q factor even *increases* on resonance. These results highlight the main conclusions of this Rapid Communication, i.e., the presence of a strong double-resonant photoelastic coupling, and the lack of a detrimental influence of exciton dephasing on the effective polariton Q factor.

On closing we center our attention on the resonant behavior on the middle polariton, shown in the right panels of Fig. 4. The dashed-dotted curves correspond to the model using the same fitting parameters as for the LP, taking $\Gamma_L = \Gamma_H$. Note the calculated double maxima, which is due to the separate almost optimum balance of S_C with either S_H or S_L. The abrupt decay of the measured Raman intensity around $\delta_H = 10$ meV results from the onset of dissipation as the polariton branch overlaps with the continuum of single-particle e-h excitations (indicated with gray background in Figs. 2 and 4), not taken into account by the model. The continuous curve is also obtained using the full calculation based on Eq. (2), but with such additional interband dissipative mechanism affecting $\Gamma_{\rm MP}$. A good description of the experiment is obtained adding *ad hoc* to $\Gamma_{\rm MP}$ a smooth function defined by a step function of Gaussian profile with typical width $\sim$0.5 meV, approaching zero at large negative detunings, and a constant value $\sim$ 1.2 meV for energies larger than the ionization edge (exciton binding energy $\sim$6.5 meV). The MP Q factor, shown in the top-right panel, strongly drops on the onset of the continuum of e-h excitations. This behavior contrasts with that displayed by the LP, and is conceptually similar to that evidenced by the Q factor of the bulk-GaAs microcavity in Fig. 1.

The magnitude of the light-sound interaction relevant to backaction can be quantified by the optomechanical coupling factor $g_{\rm om} = d\omega/du$ which describes the variation of the cavity mode angular frequency ω with the mechanical displacement u [28]. $\Omega_R = g_{\rm om}x_0$ is also used as a measure of the optomechanical coupling. Here $x_0 = \sqrt{\hbar/2m_{\rm eff}\Omega_0}$ is the zero-point motion of the mechanical oscillator, and $m_{\rm eff}$ its effective motional mass. The optomechanical coupling factor in DBR-based GaAs microcavities has been recently calculated to be $g_{\rm om}^{\rm ph} = 83$ THz/nm using a value $P = 200$ for the photoelastic constant [24]. To this purpose u is defined, as in Refs. [25,28], to be the maximum amplitude of displacement of the resonator for the specific mechanical mode under consideration (the fundamental breathing mode at 20 GHz in our case). Based on the same calculation, and assuming that a fully resonant photoelastic coupling can be attained in the strong-coupling regime (photoelastic constants in the 5×10^3 range; see Fig. 1), we thus estimate enormous optomechanical coupling factors $g_{\rm om}$ in the petaHz/nm range (petaHz $= 10^{15}$ Hz) in *polariton* optomechanics. Considering a micropillar $\lambda/2$ cavity of 1 μm radii, for the $\Omega_0 = 20$ GHz mode $m_{\rm eff} \sim 8$ pg, and thus $\Omega_R \sim 10^9$ Hz (i.e., in the $\sim$GHz range). We note that other cavity optomechanical realizations typically have $g_{\rm om}$ in the sub-GHz/nm range, and Ω_R in the hundreds of kHz.

In conclusion, we have highlighted the problem posed by dissipation to fully exploit the strong resonant dispersive photoelastic mechanism for dynamical backaction in cavity optomechanics, and demonstrated how this problem is overcome when cavity-polariton optomechanics is considered. New promising perspectives that combine the worlds of cavity optomechanics with CQED in the presence of ultrastrong optomechanical coupling can be envisaged from these results.

[1] O. Arcizet, P.-F. Cohadon, T. Briant, M. Pinard, and A. Heidmann, Nature (London) **444**, 71 (2006).
[2] T. J. Kippenberg and K. J. Vahala, Science **321**, 1172 (2008).
[3] J. D. Thompson, B. M. Zwickl, A. M. Jayich, F. Marquardt, S. M. Girvin, and J. G. E. Harris, Nature (London) **452**, 72 (2008).
[4] M. Eichenfield, J. Chan, R. M. Camacho, K. J. Vahala, and O. Painter, Nature (London) **462**, 78 (2009).
[5] M. S. Kang, A. Nazarkin, A. Brenn, and P. St. J. Russell, Nat. Phys. **5**, 276 (2009).
[6] I. Favero and K. Karrai, Nat. Photonics **3**, 201 (2009).
[7] F. Marquardt and S. M. Girvin, Physics **2**, 40 (2009).

[8] S. Gröblacher, J. B. Hertzberg, M. R. Vanner, G. D. Cole, S. Gigan, K. C. Schwab, and M. Aspelmeyer, Nature Physics **5**, 485 (2009).
[9] A. Schliesser, O. Arcizet, R. Riviere, and T. J. Kippenberg, Nat. Phys. **5**, 509 (2009).
[10] S. Weis, R. Rivière, S. Deléglise, E. Gavartin, O. Arcizet, A. Schliesser, T. J. Kippenberg, Science **330**, 1520 (2010).
[11] Q. Lin, J. Rosenberg, D. Chang, R. Camacho, M. Eichenfield, K. J. Vahala, and O. Painter, Nat. Photonics **4**, 236 (2010).
[12] A. D. O'Connell, M. Hofheinz, M. Ansmann, R. C. Bialczak, M. Lenander, E. Lucero, M. Neeley, D. Sank, H. Wang, M. Weides, J. Wenner, J. M. Martinis, and A. N. Cleland, Nature (London) **464**, 697 (2010).
[13] J. D. Teufel, T. Donner, D. Li, J. W. Harlow, M. S. Allman, K. Cicak, A. J. Sirois, J. D. Whittaker, K. W. Lehnert, and R. W. Simmonds, Nature (London) **475**, 359 (2011).
[14] J. Chan, T. P. M. Alegre, A. H. Safavi-Naeini, J. T. Hill, A. Krause, S. Gröblacher, M. Aspelmeyer, and O. Painter, Nature (London) **478**, 89 (2011).
[15] E. Verhagen, S. Deleglise, S. Weis, A. Schliesser, and T. J. Kippenberg, Nature (London) **482**, 63 (2012).
[16] C. Zhao, L. Ju, H. Miao, S. Gras, Y. Fan, and D. G. Blair, Phys. Rev. Lett. **102**, 243902 (2009).
[17] I. S. Grudinin, H. Lee, O. Painter, and K. J. Vahala, Phys. Rev. Lett. **104**, 083901 (2010).
[18] J. Restrepo, C. Ciuti, and I. Favero, Phys. Rev. Lett. **112**, 013601 (2014).
[19] O. Kyriienko, T. C. H. Liew, and I. A. Shelykh, Phys. Rev. Lett. **112**, 076402 (2014).
[20] F. Marquardt, J. P. Chen, A. A. Clerk, and S. M. Girvin, Phys. Rev. Lett. **99**, 093902 (2007).
[21] G. S. Agarwal and S. Huang, Phys. Rev. A **81**, 041803 (2010).
[22] S. Groeblacher, K. Hammerer, M. R. Vanner, and M. Aspelmeyer, Nature (London) **460**, 724 (2009).
[23] Y-C. Liu, Y-F. Xiao, Y-L. Chen, X-C. Yu, and Q. Gong, Phys. Rev. Lett. **111**, 083601 (2013).
[24] A. Fainstein, N. D. Lanzillotti-Kimura, B. Jusserand, and B. Perrin, Phys. Rev. Lett. **110**, 037403 (2013).
[25] C. Baker, W. Hease, D.-T. Nguyen, A. Andronico, S. Ducci, G. Leo, and I. Favero, Optics Express **22**, 14072 (2014).
[26] G. Bahl and T. Carmon, arXiv:1309.2828.
[27] M. Tomes and T. Carmon, Phys. Rev. Lett. **102**, 113601 (2009).
[28] L. Ding, C. Baker, P. Senellart, A. Lemaitre, S. Ducci, G. Leo, and I. Favero, Phys. Rev. Lett. **105**, 263903 (2010).
[29] A. Feldman and D. Horowitz, J. Appl. Phys. **39**, 5597 (1968).
[30] B. Jusserand, A. Fainstein, R. Ferreira, S. Majrab, and A. Lemaître, Phys. Rev. B **85**, 041302(R) (2012).
[31] N. D. Lanzillotti-Kimura, A. Fainstein, and B. Jusserand, Ultrasonics (2014), doi:10.1016/j.ultras.2014.05.017
[32] M. Gurioli, J. Martinez-Pastor, M. Colocci, A. Bosacchi, S. Franchi, and L. C. Andreani, Phys. Rev. B **47**, 15755 (1993).
[33] A. Kavokin and G. Malpuech, *Cavity Polaritons* (Elsevier, Amsterdam, 2003).
[34] C. Ciuti, P. Schwendimann, and A. Quattropani, Semicond. Sci. Technol. **18**, S279 (2003); special issue on *Microcavities*, edited by J. J. Baumberg and L. Viña.
[35] R. Houdré, R. P. Stanley, U. Oesterle, M. Ilegems, and C. Weisbuch, Phys. Rev. B **49**, 16761 (1994).
[36] R. Houdré, R. P. Stanley, and M. Ilegems, Phys. Rev. A **53**, 2711 (1996).
[37] G. Bogiovanni, A. Mura, F. Quochi, S. Gürtler, J. L. Staehli, F. Tassone, R. P. Stanley, U. Oesterle, and R. Houdré, Phys. Rev. B **55**, 7084 (1997).
[38] B. Sermage, S. Long, I. Abram, J. Y. Marzin, J. Bloch, R. Planel, and V. Thierry-Mieg, Phys. Rev. B **53**, 16516 (1996).
[39] D. M. Whittaker, P. Kinsler, T. A. Fisher, M. S. Skolnick, A. Armitage, A. M. Afshar, M. D. Sturge, J. S. Roberts, G. Hill, and M. A. Pate, Phys. Rev. Lett. **77**, 4792 (1996).
[40] A. Fainstein, B. Jusserand, and V. Thierry-Mieg, Phys. Rev. Lett. **78**, 1576 (1997).
[41] See Supplemental Material at http://link.aps.org/supplemental/10.1103/PhysRevB.90.201302 for more information on the connection between optomechanical coupling and Raman scattering, on the sample structure and luminescence, on the factorization model of polariton mediated Raman scattering applied to the discussed problem, and on the details of the observed Raman spectra.
[42] For a description of the technical difficulties involving Raman scattering at such low frequencies, see S. Anguiano, G. Rozas, A. E. Bruchhausen, A. Fainstein, B. Jusserand, P. Senellart, and A. Lemaître, Phys. Rev. B **90**, 045314 (2014).
[43] M. Trigo, A. Bruchhausen, A. Fainstein, B. Jusserand, and V. Thierry-Mieg, Phys. Rev. Lett. **89**, 227402 (2002).
[44] G. Rozas, M. F. Pascual Winter, B. Jusserand, A. Fainstein, B. Perrin, E. Semenova, and A. Lemaître, Phys. Rev. Lett. **102**, 015502 (2009).
[45] M. M. de Lima, Jr., M. van der Poel, P. V. Santos, and J. M. Hvam, Phys. Rev. Lett. **97**, 045501 (2006).
[46] E. A. Cerda-Mendez, D. N. Krizhanovskii, M. Wouters, R. Bradley, K. Biermann, K. Guda, R. Hey, P. V. Santos, D. Sarkar, and M. S. Skolnick, Phys. Rev. Lett. **105**, 116402 (2010).
[47] T. Berstermann, A. V. Scherbakov, A. V. Akimov, D. R. Yakovlev, N. A. Gippius, B. A. Glavin, I. Sagnes, J. Bloch, and M. Bayer, Phys. Rev. B **80**, 075301 (2009).
[48] A. Fainstein, B. Jusserand, and V. Thierry-Mieg, Phys. Rev. Lett. **75**, 3764 (1995).
[49] A. Fainstein and B. Jusserand, Phys. Rev. B **57**, 2402 (1998).
[50] B. Jusserand and M. Cardona, in *Light Scattering in Solids V*, edited by M. Cardona and G. Güntherodt (Springer, Berlin, 1982).
[51] A. Fainstein and B. Jusserand, in *Light Scattering in Solids IX*, edited by M. Cardona and R. Merlin (Springer, Heidelberg, 2007).
[52] J. He, B. Djafari-Rouhani, and J. Sapriel, Phys. Rev. B **37**, 4086 (1988).
[53] M. Trigo, A. Fainstein, B. Jusserand, and V. Thierry-Mieg, Phys. Rev. B **66**, 125311 (2002).
[54] B. Bendow and J. L. Birman, Phys. Rev. B **1**, 1678 (1970); B. Bendow, *ibid.* **2**, 5051 (1970); See also , in *Polariton Theory of Resonance Raman Scattering in Solids*, Springer Tracts in Modern Physics Vol. 82 (Springer, Berlin, 1978).
[55] M. Matsushita, J. Wicksted, and H. Z. Cummins, Phys. Rev. B **29**, 3362 (1984); M. Matsushita and M. Nakayama, *ibid.* **30**, 2074 (1984).
[56] C. Weisbuch and R. G. Ulbrich, in *Light Scattering in Solids III*, edited by M. Cardona and G. Güntherodt (Springer, Berlin, 1989).
[57] A. Bruchhausen, L. M. León Hilario, A. A. Aligia, A. M. Lobos, A. Fainstein, B. Jusserand, and R. André, Phys. Rev. B **78**, 125326 (2008).